Weak Formulations for Finite Element Analysis of an Electromagnetic Eigenvalue Problem

By Fumio KIKUCHI

Department of Mathematics, College of Arts and Sciences,
University of Tokyo

(Received August 25, 1988)

Abstract

This paper presents some weak (or variational) formulations for an electromagnetic eigenvalue problem related to the analysis of cavity resonators in microwave theory. Particularly, mixed and penalty formulations are considered, since they appear to be applicable to finite element analysis of such a problem. Moreover, some theoretical results are derived for these formulations. Then, a simple two-dimensional finite element is developed by the penalty formulation, and tested by numerical computations. We point out some numerical difficulties observed in this type of piecewise polynomial finite elements based on the penalty approach.

Key words: electromagnetics, resonators, eigenvalue problem, FEM, mixed method, penalty method.

§ 1. Introduction

Let Ω be a bounded domain in $\boldsymbol{R}^3$ with Lipschitz continuous boundary $\partial\Omega$. In the microwave theory such as adopted in particle accelerator physics [1], we often consider an eigenvalue problem for a non-negative number λ (eigenvalue) and a real vector-valued function $\vec{E}$ (eigenfunction): find a pair $\{\lambda, \vec{E}\}$ such that $\vec{E}\neq\vec{0}$ and

$$\operatorname{rot}\operatorname{rot}\vec{E}=\lambda\vec{E}, \quad \operatorname{div}\vec{E}=0 \ \text{ in } \Omega; \quad \vec{E}\times\vec{n}=\vec{0} \ \text{ on } \partial\Omega, \tag{1}$$

where $\vec{n}$ denotes the outward unit normal on $\partial\Omega$ and $\times$ does the vector product. Physically, $\vec{E}$ represents the amplitude of a time-harmonic electric field, and λ is a quantity proportional to the square of the frequency of the time-harmonic vibration. The boundary condition in (1) means that the boundary $\partial\Omega$ consists of a perfect conductor, and an additional boundary condition $\operatorname{div}\vec{E}=0$ is sometimes imposed there.

If the amplitude of a magnetic field $\vec{H}$ is employed as the fundamental quantity in place of $\vec{E}$, the present problem becomes

$$\left.\begin{aligned} &\operatorname{rot}\operatorname{rot}\vec{H}=\lambda\vec{H}, \quad \operatorname{div}\vec{H}=0 \quad \text{in } \Omega \\ &\vec{H}\cdot\vec{n}=0, \quad (\operatorname{rot}\vec{H})\times\vec{n}=\vec{0} \quad \text{on } \partial\Omega \end{aligned}\right\}. \tag{2}$$

Physically, the equivalence of these two problems is known for positive values of λ: we will later give a mathematical proof in the framework of the Hilbert space method (Theorem 2).

A difficulty of this problem is how to deal with the *divergence-free condition*: $\operatorname{div}\vec{E}=0$. However, if $\vec{E}$ satisfies the first relation in (1) for $\lambda\neq 0$, this condition holds automatically for such $\vec{E}$ since $\operatorname{div}\vec{E}=\lambda^{-1}\operatorname{div}(\operatorname{rot}\operatorname{rot}\vec{E})=0$. Thus, the divergence-free condition is consistent with the first relation so long as we are interested in time-harmonic electric fields with $\lambda>0$. This fact will be also proved in this paper (Theorem 1). Another difficulty is the complexity of function spaces appearing in the weak formulations of the present problem as we will see later: we need some Hilbert spaces other than the Sobolev spaces to describe the present problem mathematically.

Recently, three-dimensional calculations of electromagnetic problems become increasingly important. Unlike in the two-dimensional cases, the basis of such calculations does not appear to be fully developed at present. As a theoretical study for such an aim, we will first give some mathematical preliminaris (Section 2), and then derive some weak formulations for the above problem (Section 3): in particular, mixed and penalty formulations will be discussed, since they appear to be theoretically interesting and practically promising. Moreover, we will present a simple two-dimensional finite element model based on the penalty approach and test it numerically by a few sample problems (Sections 4 and 5). It is a classical "nodal point" element based on the piecewise linear Lagrange interpolation polynomial. In particular, we will point out some numerical difficulties of such an element when Ω has an reentrant corner. This type of numerical phenomenon appears to be commonly observed when the penalty approach is used with the usual piecewise polynomial approximate functions, see also [14].

The results of this paper are partially announced in [12] without proofs, where some numerical results based on the Nedelec finite element spaces [16, 17] are also included.

§ 2. Function spaces and preliminary results

Let Ω be a bounded domain in $\boldsymbol{R}^3$ with Lipschitz continuous boundary. Let us consider some real function spaces related to Ω. First, $H^1(\Omega)$ and $H_0^1(\Omega)$ are the usual first-order Sobolev spaces, and $L_2(\Omega)$ is the L_2-space for Ω. We will denote by $(\cdot,\cdot)$ the inner product of $L_2(\Omega)$ or $\{L_2(\Omega)\}^3$. Similarly, we will use $\|\cdot\|$ to denote the norm of $L_2(\Omega)$ or $\{L_2(\Omega)\}^3$. Moreover, we define

$$H_C^1(\Omega)=\{q\in H^1(\Omega);\ \text{the trace of } q \text{ is constant on each connected component of } \partial\Omega\}. \tag{3}$$

Note that $H^1(\Omega)$, $H_0^1(\Omega)$, and $H_C^1(\Omega)$ are Hilbert spaces, and that the latter two are subspaces of the first.

We also use some real Hilbert spaces of vector functions for electromagnetic fields, see e. g. [5, 6]. We first introduce three Hilbert spaces with their norms.

$$H(\mathrm{rot}\,;\Omega)=\{v\in\{L_2(\Omega)\}^3\,;\ \mathrm{rot}\,v\in\{L_2(\Omega)\}^3\}\ \text{equipped with}$$
$$\|v\|_{H(\mathrm{rot}\,;\Omega)}=(\|v\|^2+\|\mathrm{rot}\,v\|^2)^{1/2}\,, \tag{4}$$

$$H(\mathrm{div}\,;\Omega)=\{v\in\{L_2(\Omega)\}^3\,;\ \mathrm{div}\,v\in L_2(\Omega)\}\ \text{equipped with}$$
$$\|v\|_{H(\mathrm{div}\,;\Omega)}=(\|v\|^2+\|\mathrm{div}\,v\|^2)^{1/2}\,, \tag{5}$$

$$H(\mathrm{rot}\,;\Omega)\cap H(\mathrm{div}\,;\Omega)=\{v\in\{L_2(\Omega)\}^3\,;\ \mathrm{rot}\,v\in\{L_2(\Omega)\}^3,\ \mathrm{div}\,v\in L_2(\Omega)\}\ \text{equipped with}$$
$$\|v\|_{H(\mathrm{rot}\,;\Omega)\cap H(\mathrm{div}\,;\Omega)}=(\|v\|^2+\|\mathrm{rot}\,v\|^2+\|\mathrm{div}\,v\|^2)^{1/2}\,. \tag{6}$$

Here, *rot* and *div* are the usual differential operators in the sense of distribution. Later, the gradient operator *grad* will be also used. The inner products of the above Hilbert spaces are the standard ones associated with the norms. These function spaces are not the usual Sobolev spaces. Clearly, $\{H^1(\Omega)\}^3$ is continuously imbedded in $H(\mathrm{rot}\,;\Omega)\cap H(\mathrm{div}\,;\Omega)$: the converse is, however, not true in general [20].

The following spaces are subspaces of $H(\mathrm{rot}\,;\Omega)$ or $H(\mathrm{div}\,;\Omega)$.

$$H_0(\mathrm{rot}\,;\Omega)=\{v\in H(\mathrm{rot}\,;\Omega)\,;\ (v,\mathrm{rot}\,\phi)=(\mathrm{rot}\,v,\phi)\ \text{for all}\ \phi\in H(\mathrm{rot}\,;\Omega)\}\,, \tag{7}$$

$$H(\mathrm{rot}^0\,;\Omega)=\{v\in H(\mathrm{rot}\,;\Omega)\,;\ \mathrm{rot}\,v=0\}=\{v\in\{L_2(\Omega)\}^3\,;\ (v,\mathrm{rot}\,\phi)=0\ \text{for all}\ \phi\in H_0(\mathrm{rot}\,;\Omega)\}\,, \tag{8}$$

$$H_0(\mathrm{rot}^0\,;\Omega)=\{v\in H_0(\mathrm{rot}\,;\Omega)\,;\ \mathrm{rot}\,v=0\}=\{v\in\{L_2(\Omega)\}^3\,;\ (v,\mathrm{rot}\,\phi)=0\ \text{for all}\ \phi\in H(\mathrm{rot}\,;\Omega)\}\,, \tag{9}$$

$$H_0(\mathrm{div}\,;\Omega)=\{v\in H(\mathrm{div}\,;\Omega)\,;\ (v,\mathrm{grad}\,q)=-(\mathrm{div}\,v,q)\ \text{for all}\ q\in H^1(\Omega)\}\,, \tag{10}$$

$$H(\mathrm{div}^0\,;\Omega)=\{v\in H(\mathrm{div}\,;\Omega)\,;\ \mathrm{div}\,v=0\}=\{v\in\{L_2(\Omega)\}^3\,;\ (v,\mathrm{grad}\,q)=0\ \text{for all}\ q\in H_0^1(\Omega)\}\,, \tag{11}$$

$$H_0(\mathrm{div}^0\,;\Omega)=\{v\in H_0(\mathrm{div}\,;\Omega)\,;\ \mathrm{div}\,u=0\}=\{v\in\{L_2(\Omega)\}^3\,;\ (v,\mathrm{grad}\,q)=0\ \text{for all}\ q\in H^1(\Omega)\}\,. \tag{12}$$

The meaning of $v\in H_0(\mathrm{rot}\,;\Omega)$ is that $v\in H(\mathrm{rot}\,;\Omega)$ and the tangential components of v on $\partial\Omega$ vanish in a generalized sense [5, 6]. Similarly, $v\in H_0(\mathrm{div}\,;\Omega)$ if and only if $v\in H(\mathrm{div}\,;\Omega)$ and the normal component of v on $\partial\Omega$ vanishes in a generalized sense.

Let us list some important results on these spaces.

(i) $\operatorname{grad} q \in H(\mathrm{rot}^0; \Omega)$ for each $q \in H^1(\Omega)$.

(ii) $\operatorname{grad} q \in H_0(\mathrm{rot}^0; \Omega)$ for each $q \in H_C^1(\Omega)$.

(iii) If Ω is simply-connected, there exists for each $v \in H(\mathrm{rot}^0; \Omega)$ a function $q \in H^1(\Omega)$ such that $\operatorname{grad} q = v$. Such q is unique up to an additive constant.

(iv) For each $v \in H_0(\mathrm{rot}^0; \Omega)$, there exists $q \in H_C^1(\Omega)$ such that $\operatorname{grad} q = v$. In particular, when $\partial\Omega$ is connected, q can be taken uniquely from $H_0^1(\Omega)$.

For (ii) and (iii), see Theorem 2.9 and the proof of Theorem 3.4 of [6]. On the other hand, (i) is trivial, and (iv) can be derived from (iii) by extending $v \in H_0(\mathrm{rot}^0; \Omega)$ as zero outside Ω.

We will use the following notations:

$$\left.\begin{array}{ll} U_1 = H_0(\mathrm{rot}; \Omega), & U_2 = H(\mathrm{rot}; \Omega), \\ V_1 = U_1 \cap H(\mathrm{div}; \Omega), & V_2 = U_2 \cap H_0(\mathrm{div}; \Omega), \\ W_1 = H_0^1(\Omega), & W_2 = H^1(\Omega), \end{array}\right\} \tag{13}$$

where V_1 and V_2 are subspaces of $H(\mathrm{rot}; \Omega) \cap H(\mathrm{div}; \Omega)$.

By means of the Poincare-Friedrichs inequalities, $\operatorname{grad} H_0^1(\Omega)$ and $\operatorname{grad} H^1(\Omega)$ may be considered closed subspaces of U_1 and U_2, respectively, where $\operatorname{grad} H_0^1(\Omega) = \{v = \operatorname{grad} q;\ q \in H_0^1(\Omega)\}$, for example. Then due to (11) and (12), we have the following *orthogonal decompositions* of U_i and V_i for $i = 1, 2$:

$$U_1 = \{U_1 \cap H(\mathrm{div}^0; \Omega)\} \oplus \operatorname{grad} H_0^1(\Omega), \tag{14}$$

$$U_2 = \{U_2 \cap H_0(\mathrm{div}^0; \Omega)\} \oplus \operatorname{grad} H^1(\Omega), \tag{15}$$

$$V_i = \{V_i \cap H(\mathrm{div}^0; \Omega)\} \oplus (V_i \cap \operatorname{grad} W_i) \qquad (i = 1, 2). \tag{16}$$

Notice that $\operatorname{grad} H_0^1(\Omega) \subset H_0(\mathrm{rot}^0; \Omega)$ and $\operatorname{grad} H^1(\Omega) \subset H(\mathrm{rot}^0; \Omega)$ from (i) and (ii). Moreover, we find from (iii) and (iv) that

$$\operatorname{grad} H_0^1(\Omega) = H_0(\mathrm{rot}^0; \Omega) \quad \text{when } \partial\Omega \text{ is connected,} \tag{17}$$

$$\operatorname{grad} H^1(\Omega) = H(\mathrm{rot}^0; \Omega) \quad \text{when } \Omega \text{ is simply-connected.} \tag{18}$$

Note that the boundaries of cavity resonators are usually connected and then (17) holds.

As in [13], let us consider the rotation operator in two settings:

$$S_i : U_i \to \{L_2(\Omega)\}^3;\ S_i u = \mathrm{rot}\, u \quad \text{for } u \in U_i \qquad (i = 1, 2). \tag{19}$$

As usual, the dual operator of S_i is denoted by $S_i^* : \{L_2(\Omega)\}^3 \to U_i$ $(i = 1, 2)$. Furthermore, the null space and the range of a linear operator are designated by $N(\cdot)$ and $R(\cdot)$, respectively. Then we have the following orthogonal decompositions for $i = 1, 2$:

$$U_i = N(S_i) \oplus \overline{R(S_i^*)}, \qquad \{L_2(\Omega)\}^3 = N(S_i^*) \oplus \overline{R(S_i)}, \tag{20}$$

where $\overline{R(S_i^*)}$, for example, denotes the closure of $R(S_i^*)$ in U_i. As is shown in

[13], we have

$$N(S_1)=H_0(\mathrm{rot}^0;\Omega),\qquad N(S_2)=H(\mathrm{rot}^0;\Omega), \tag{21}$$

$$N(S_1^*)=H(\mathrm{rot}^0;\Omega)=N(S_2),\qquad N(S_2^*)=H_0(\mathrm{rot}^0;\Omega)=N(S_1), \tag{22}$$

$$R(S_1)\subset H_0(\mathrm{div}^0;\Omega),\qquad R(S_2)\subset H(\mathrm{div}^0;\Omega), \tag{23}$$

$$\overline{R(S_1)}=H_0(\mathrm{div}^0;\Omega)\quad \text{if } \Omega \text{ is simply-connected}, \tag{24}$$

$$\overline{R(S_2)}=H(\mathrm{div}^0;\Omega)\quad \text{if } \partial\Omega \text{ is connected}, \tag{25}$$

$$R(S_i^*)\subset V_i\cap H(\mathrm{div}^0;\Omega)\qquad (i=1,2), \tag{26}$$

$$\overline{R(S_1^*)}=U_1\cap\overline{R(S_2)},\qquad \overline{R(S_2^*)}=U_2\cap\overline{R(S_1)}, \tag{27}$$

$$\overline{R(S_1^*)}=H_0(\mathrm{rot};\Omega)\cap H(\mathrm{div}^0;\Omega)\quad \text{if } \partial\Omega \text{ is connected}, \tag{28}$$

$$\overline{R(S_2^*)}=H(\mathrm{rot};\Omega)\cap H_0(\mathrm{div}^0;\Omega)\quad \text{if } \Omega \text{ is simply-connected}. \tag{29}$$

We can also obtain the following orthogonal decompositions with respect to the inner product of $H(\mathrm{rot};\Omega)$ or $H(\mathrm{rot};\Omega)\cap H(\mathrm{div};\Omega)$.

$$H_0(\mathrm{rot};\Omega)\cap H(\mathrm{div}^0;\Omega)=\overline{R(S_1^*)}\oplus\{H_0(\mathrm{rot}^0;\Omega)\cap H(\mathrm{div}^0;\Omega)\}, \tag{30}$$

$$H(\mathrm{rot};\Omega)\cap H_0(\mathrm{div}^0;\Omega)=\overline{R(S_2^*)}\oplus\{H(\mathrm{rot}^0;\Omega)\cap H_0(\mathrm{div}^0;\Omega)\}. \tag{31}$$

In order to assure the closedness of the ranges appearing above and also to use for some other purposes, we employ the following two assumptions [H1] and [H2].

[Hi] $\quad V_i$ is compactly imbedded in $\{L_2(\Omega)\}^3$ $(i=1,2)$.

REMARK 1. [H1] and [H2] both hold when Ω is a bounded domain with sufficiently smooth boundary or Ω is a convex bounded domain, since V_1 and V_2 are continuously imbedded in $\{H^1(\Omega)\}^3$ in such cases, see [5, 6, 10, 11]. Moreover, according to Weck [20], [H1] holds when Ω is a "C-region". □

As is shown in [13], a direct consequence of [Hi] is that $R(S_i)$ *and* $R(S_i^*)$ *are respectively closed in* $\{L_2(\Omega)\}^3$ *and* U_i $(i=1,2)$. We can also see that $R(S_1)$ is closed in $\{L_2(\Omega)\}^3$ if and only if $R(S_2)$ is closed in $\{L_2(\Omega)\}^3$, by noting that S_1 and S_2 are the dual operators of each other when they are considered (unbounded) operators in $\{L_2(\Omega)\}^3$.

Let us list two results related to [H1] and [H2], whose proofs are quite similar to each other and given later.

(v) $\overline{R(S_2^*)}$ as a subspace of V_2 is compactly imbedded in $\{L_2(\Omega)\}^3$ if and only if $\overline{R(S_1^*)}$ as a subspace of V_1 is compactly imbedded in $\{L_2(\Omega)\}^3$.

(vi) If $V_i\cap H(\mathrm{div}^0;\Omega)$ as a subspace of V_i is compactly imbedded in $\{L_2(\Omega)\}^3$,

then [Hi] holds true ($i=1, 2$).

REMARK 2. If [H1] holds, then $R(S_1^*)\subset V_1$ is closed and is compactly imbedded in $\{L_2(\Omega)\}^3$. Thus, if Ω is simply-connected in addition, then $R(S_2^*)=H(\mathrm{rot}\,;\Omega)\cap H_0(\mathrm{div}^0\,;\Omega)=V_2\cap H(\mathrm{div}^0\,;\Omega)$ from (29), and hence [H2] holds due to (v) and (vi). Moreover, if $H(\mathrm{rot}^0\,;\Omega)\cap H_0(\mathrm{div}^0\,;\Omega)$ is shown to be finite-dimensional even when Ω is not simply-connected, then [H2] follows from [H1] due to (31). Of course, $H(\mathrm{rot}^0\,;\Omega)\cap H_0(\mathrm{div}^0\,;\Omega)$ is finite-dimensional when [H2] holds. Similarly, if [H2] holds and $\partial\Omega$ is connected, then $R(S_1^*)=H_0(\mathrm{rot}\,;\Omega)\cap H(\mathrm{div}^0\,;\Omega)=V_1\cap H(\mathrm{div}^0\,;\Omega)$ from (28), and hence [H1] holds. In this case, however, [H1] follows from [H2] even when $\partial\Omega$ is not connected, since we can show from (iv) that $H_0(\mathrm{rot}^0\,;\Omega)\cap H(\mathrm{div}^0\,;\Omega)$ in (30) is finite-dimensional (that is, the number of connected components of $\partial\Omega$ is finite) under the present assumptions on Ω. □

(a) *Proof of* (v). We will only prove the "if" part: the "only if" part may be proved similarly. If $\overline{R(S_1^*)}$ as a subspace of V_1 is compactly imbedded in $\{L_2(\Omega)\}^3$, then $R(S_1)$ and $R(S_1^*)$ are closed respectively in $\{L_2(\Omega)\}^3$ and U_1, and we have $\overline{R(S_2^*)}=U_2\cap R(S_1)$ from (27). Let us consider a sequence $\{u_n\}_{n=1}^{\infty}$ in $\overline{R(S_2^*)}$ such that $\|u_n\|_{V_2}$ $(=\|u_n\|_{U_2})\leqq 1$ $(n=1, 2, \cdots)$. Clearly, there exists a subsequence $\{u_n^*\}_{n=1}^{\infty}$ of $\{u_n\}_{n=1}^{\infty}$ that converges weakly in U_2 to a certain $u_0\in\overline{R(S_2^*)}$. Note that, for each u_n^*, there exists a unique $v_n\in R(S_1^*)$ such that $S_1v_n=\mathrm{rot}\,v_n=u_n^*$. Since $R(S_1)$ is closed in $\{L_2(\Omega)\}^3$ and v_n belongs to $R(S_1^*)$ with $\|\mathrm{rot}\,v_n\|=\|u_n^*\|\leqq 1$, we find that $\|v_n\|_{V_1}=\|v_n\|_{U_1}$ is uniformly bounded with respect to n. Thus, we can use the assumption to show that v_n converges weakly in V_1 and strongly in $\{L_2(\Omega)\}^3$ to a unique $v_0\in R(S_1^*)$ such that $\mathrm{rot}\,v_0=u_0$. Noting that $v_n\in U_1$, we now find that

$$(u_n^*, u_n^*)=(\mathrm{rot}\,v_n, u_n^*)=(v_n, \mathrm{rot}\,u_n^*)\,,$$

which converges to $(v_0, \mathrm{rot}\,u_0)=(\mathrm{rot}\,v_0, u_0)=(u_0, u_0)$ as $n\to\infty$. This fact means that u_n^* converges strongly to u_0 in $\{L_2(\Omega)\}^3$, and the proof is complete.

(b) *Proof of* (vi). The proof is given only for $i=2$, since that for $i=1$ is easier. From (16), it is sufficient to prove that $V_2\cap\mathrm{grad}\,W_2$ is compactly imbedded in $\{L_2(\Omega)\}^3$. The proof is quite similar to that of (v), and hence we only show the outline. Let us consider a sequence $\{u_n\}_{n=1}^{\infty}$ in $V_2\cap\mathrm{grad}\,W_2$ such that $\|u_n\|_{V_2}\leqq 1$. Then there exists a subsequence $\{u_n^*\}_{n=1}^{\infty}$ that converges weakly in V_2 to $u_0\in V_2$. For each u_n^*, there exists a unique $p_n\in W_2=H^1(\Omega)$ such that $\mathrm{grad}\,p_n=u_n^*$ and $(p_n, 1)=0$. Then, by the Friedrichs inequality and the Rellich theorem of choice, p_n converges weakly in W_2 and strongly in $L_2(\Omega)$ to a unique $p_0\in W_2$ such that $\mathrm{grad}\,p_0=u_0$ and $(p_0, 1)=0$. Then, as in the proof of (v), we can show that $(u_n^*, u_n^*)=-(p_n, \mathrm{div}\,u_n^*)$ converges to $-(p_0, \mathrm{div}\,u_0)=(u_0, u_0)$ as $n\to\infty$, and the proof is complete.

§ 3. Weak formulations

This section is devoted to presenting some weak formulations to the cavity resonator problem (1) or (2), the former and the latter being expressed in terms of $\vec{E}$ and $\vec{H}$, respectively. Hereafter, we will consider two sequences of formulations, the first ($i=1$) and the second ($i=2$) of which correspond to (1) and (2), respectively.

A natural formulation is given as follows for $i=1,2$:

$[\mathrm{F1}]_i$ *Find* $\{\lambda, u\}\in \boldsymbol{R}^1\times U_i$ *such that* $u\neq 0$ *and*

$$\begin{cases} (\mathrm{rot}\, u, \mathrm{rot}\, v)=\lambda(u, v)\,; & \forall v\in U_i\,, \\ (u, \mathrm{grad}\, q)=0 \quad\ ; & \forall q\in W_i\,. \end{cases} \tag{32}$$

The first relation of the above means that $\mathrm{rot}\,\mathrm{rot}\, u=\lambda u$, and that, for $i=2$, the tangential components of $\mathrm{rot}\, u$ vanish on $\partial\Omega$ due to (7). Moreover, for $i=1$, the boundary condition for $\vec{E}$ in (1) is taken into account as the condition $u\in U_1$. Similarly, the second condition above means that $u\in H(\mathrm{div}^0\,;\Omega)$ for $i=1$ and $u\in H_0(\mathrm{div}^0\,;\Omega)$ for $i=2$. That is, it means that $\mathrm{div}\, u=0$ and that, for $i=2$, the normal component of u vanishes on $\partial\Omega$. Thus all the relations in (1) and (2) are taken account of in the present formulation. Furthermore, under [H1] and [H2], the spectral problems associated with $[\mathrm{F1}]_{i=1,2}$ have nice properties: the spectra consist of eigenvalues only and have no accumulation points except infinity, each eigenvalue is non-negative and is at most finitely degenerate, and some typical expansion theorems are valid.

As was pointed out in Section 1, the second condition of (32) may be omitted if we consider non-zero eigenvalues only:

THEOREM 1. *For* $\lambda\neq 0$ *and* $i=1, 2$, *consider* $u\in U_i$ *such that*

$$(\mathrm{rot}\, u, \mathrm{rot}\, v)=\lambda(u, v)\,; \quad \forall v\in U_i\,. \tag{33}$$

Then u *satisfies*

$$(u, \mathrm{grad}\, q)=0\,; \quad \forall q\in W_i\,. \tag{34}$$

Proof. Let us consider $v=\mathrm{grad}\, q$ for $q\in W_i$. Then by (i) and (ii), $v\in U_i\cap H(\mathrm{rot}^0\,;\Omega)$. Substituting this v into (33), we find that $\lambda(u, \mathrm{grad}\, q)=0$, from which the conclusion follows. □

Despite the above results, finite element models omitting the second condition of (32) usually suffer from the spectral pollution [7] since U_i is not compactly imbedded in $\{L_2(\Omega)\}^3$. In fact, 0 is now an infinitely degenerate eigenvalue whose eigenspace is $U_i\cap H(\mathrm{rot}^0\,;\Omega)$.

We can also see that $[\mathrm{F1}]_1$ and $[\mathrm{F1}]_2$ are in a sense equivalent to each other

so long as we consider only non-zero eigenvalues and their associated eigenfunctions (this fact is physically well known, as was noted in Section 1).

THEOREM 2. *Let us consider* $\{\lambda, u\}\in \boldsymbol{R}^1\times U_1$ *such that*

$$(\mathrm{rot}\, u, \mathrm{rot}\, v)=\lambda(u, v)\,;\quad \forall v\in U_1\,. \tag{35}$$

Then $u^*=\mathrm{rot}\, u$ *belongs to* U_2 *and satisfies*

$$(\mathrm{rot}\, u^*, \mathrm{rot}\, v)=\lambda(u^*, v)\,;\quad \forall v\in U_2\,. \tag{36}$$

Conversely, let us consider $\{\lambda, u^*\}\in \boldsymbol{R}^1\times U_2$ *that satisfies* (36). *Then* $u=\mathrm{rot}\, u^*$ *belongs to* U_1 *and satisfies* (35).

Proof. 1. Let us first prove the former part of the theorem. It may be readily seen from (35) that $u^*=\mathrm{rot}\, u\in\{L_2(\Omega)\}^3$ satisfies $\mathrm{rot}\, u^*=\mathrm{rot}\,\mathrm{rot}\, u=\lambda u\in\{L_2(\Omega)\}^3$, and hence $u^*\in H(\mathrm{rot}\,;\Omega)=U_2$. Moreover, for $v\in U_2$, we have

$$(\mathrm{rot}\, u^*, \mathrm{rot}\, v)=\lambda(u, \mathrm{rot}\, v)=\lambda(\mathrm{rot}\, u, v)=\lambda(u^*, v)$$

since $u\in U_1=H_0(\mathrm{rot}\,;\Omega)$. Thus we have proved the former part.

2. To prove the latter part, let us consider $u^*\in U_2$ subjected to (36). Then we can easily show that $u=\mathrm{rot}\, u^*$ belongs to $H(\mathrm{rot}\,;\Omega)$ with $\mathrm{rot}\, u=\mathrm{rot}\,\mathrm{rot}\, u^*=\lambda u^*$. Moreover, for $v\in H(\mathrm{rot}\,;\Omega)$,

$$(u, \mathrm{rot}\, v)=(\mathrm{rot}\, u^*, \mathrm{rot}\, v)=\lambda(u^*, v)=(\mathrm{rot}\, u, v)\,,$$

and hence $u\in H_0(\mathrm{rot}\,;\Omega)=U_1$. Finally, for $v\in U_1$, we have

$$(\mathrm{rot}\, u, \mathrm{rot}\, v)=\lambda(u^*, \mathrm{rot}\, v)=\lambda(\mathrm{rot}\, u^*, v)=\lambda(u, v)\,,$$

and the proof is complete. □

A major difficulty of $[\mathrm{F1}]_i$ when they are applied to the finite element method lies in the second condition of (32). A typical method to relax such a constraint condition is the *mixed formulation* based on the Lagrange multiplier [3].

$[\mathrm{F2}]_i$ *Find* $\{\lambda, u, p\}\in \boldsymbol{R}^1\times U_i\times W_i$ *such that* $u\neq 0$ *and*

$$\begin{cases} (\mathrm{rot}\, u, \mathrm{rot}\, v)+(\mathrm{grad}\, p, v)=\lambda(u, v)\,; & \forall v\in U_i\,, \\ (u, \mathrm{grad}\, q)=0 \qquad\qquad\qquad\quad\ ; & \forall q\in W_i\,. \end{cases} \tag{37}$$

Here, p is the Lagrange multiplier introduced to deal with the linear constraint condition. Clearly, any eigenpair of $[\mathrm{F1}]_i$ with $p=0$ satisfies (37). Conversely, $\mathrm{grad}\, p$ in (37) is found to be zero by equating v to $\mathrm{grad}\, p\in U_i\cap H(\mathrm{rot}^0\,;\Omega)$ in the first relation. Thus $[\mathrm{F2}]_i$ is equivalent to $[\mathrm{F1}]_i$.

We can also consider the following perturbation problem of $[\mathrm{F2}]_i$ by intro-

ducing a (small) positive parameter ε.

$[F3]_i$ *Fix* $\varepsilon>0$, *and find* $\{\lambda, u, p\}\in \boldsymbol{R}^1\times U_i\times W_i$ *such that* $u\neq 0$ *and*

$$\begin{cases} (\mathrm{rot}\, u, \mathrm{rot}\, v)+(\mathrm{grad}\, p, v)=\lambda(u, v)\,; & \forall v\in U_i\,, \\ (u, \mathrm{grad}\, q)-\varepsilon(p, q)=0 \qquad\quad ; & \forall q\in W_i\,. \end{cases} \tag{38}$$

Clearly, any eigenpair of $[F2]_i$ is that of $[F3]_i$, but there may exist eigenpairs of $[F3]_i$ other than those of $[F2]_i$.

For the selection of the parameter $\varepsilon>0$, we have the following results, which mean that we need not use too small values of ε if we are interested in a fairly restricted number of eigenpairs as is often the case in practical applications.

THEOREM 3. *Let* λ_0 *be an arbitrary fixed positive number. Then any eigenvalue of* $[F3]_i$ *in the interval* $]0, \lambda_0]$, *if it exists, is necessarily an eigenvalue of* $[F1]_i$ *provided that*

$$0<\varepsilon<\mu_i/\lambda_0\,, \tag{39}$$

where μ_i *is the smallest positive eigenvalue of the eigenvalue problem* $(i=1, 2)$: *find* $\{\mu, r\}\in \boldsymbol{R}^1\times W_i$ *such that* $r\neq 0$ *and*

$$(\mathrm{grad}\, r, \mathrm{grad}\, q)=\mu(r, q)\,; \quad \forall q\in W_i\,. \tag{40}$$

Proof. Equating v in (38) to $\mathrm{grad}\, q$ for $q\in W_i$, we have

$$(\mathrm{grad}\, p, \mathrm{grad}\, q)=\lambda(u, \mathrm{grad}\, q)=\lambda\varepsilon(p, q) \quad (\forall q\in W_i)\,,$$

which implies that either p is zero or $\lambda\varepsilon>0$ is an eigenvalue of (40). However, $\lambda\varepsilon$ cannot be an eigenvalue of (40) since $0<\lambda\varepsilon\leqq\lambda_0\varepsilon<\mu_i$ from (39). Thus we find $p=0$, and then $[F3]_i$ reduces to $[F2]_i$ (or $[F1]_i$). That is, the considered eigenvalue of $[F3]_i$ is also that of $[F1]_i$. □

Another approach to deal with the second condition in (32) is the *penalty method*, in which $\varepsilon>0$ is again used.

$[F4]_i$ *Fix* $\varepsilon>0$, *and find* $\{\lambda, u\}\in \boldsymbol{R}^1\times V_i$ *such that* $u\neq 0$ *and*

$$(\mathrm{rot}\, u, \mathrm{rot}\, v)+\varepsilon^{-1}(\mathrm{div}\, u, \mathrm{div}\, v)=\lambda(u, v)\,; \quad \forall v\in V_i\,. \tag{41}$$

An advantage of the penalty approach is that we need not use any additional quantities such as p. However, the function spaces for u are different from those for u used in the other formulations. The penalty approach was employed by Leis [15] for boundary value problems of electromagnetic waves, and ε (or its inverse) is called the *penalty parameter*.

By means of the Fredholm alternative and the theory of mixed formulation,

we can show for each $\varepsilon>0$ that $[F3]_i$ is equivalent to $[F4]_i$ with $p=-\varepsilon^{-1}\operatorname{div} u$. Thus Theorem 3 also applies to $[F4]_i$. Note also that $\operatorname{div} u\in W_i$. The details of the present discussion may be found in [13] and are omitted here.

§ 4. A penalty finite element method for 2-D problems

As applications of our weak formulations to numerical analysis, we considered a mixed finite element method based on $[F2]_i$ in [9, 12], and also a penalty finite element method based on $[F4]_i$ in [8, 14]. In this section, we will reconsider the penalty finite element method especially in 2-D (two-dimensional) cases.

In the penalty finite element method, we first prepare a suitable finite-dimensional subspace V_i^h of V_i $(i=1, 2)$. Then the approximate problem is given by:

$[F4]_i^h$ *Fix* $\varepsilon>0$, *and find* $\{\lambda_h, u_h\}\in \boldsymbol{R}^1\times V_i^h$ *such that* $u_h\neq 0$ *and*

$$(\operatorname{rot} u_h, \operatorname{rot} v_h)+\varepsilon^{-1}(\operatorname{div} u_h, \operatorname{div} v_h)=\lambda_h(u_h, v_h)\,;\quad \forall v_h\in V_i^h\,. \tag{42}$$

To discuss the convergence of the penalty approach, we usually consider a family of finite-dimensional subspaces $\{V_i^h\}_{h>0}$ constructed over a regular family of triangulations of Ω, where h denotes the maximum diameter of finite elements in each triangulation. Then, if the penalty parameter $\varepsilon>0$ is fixed, a sufficient condition for convergence under [Hi] is given by the following *approximation capability* for the family of subspaces $\{V_i^h\}_{h>0}$ of V_i.

For each $v\in V_i$, *there exists a family* $\{v_h\}_{h>0}$ *such that* $v_h\in V_i^h$ *for each* $h>0$ *and satisfies*

$$\lim_{h\downarrow 0}\|v_h-v\|_{V_i}=0\,. \tag{43}$$

Under the assumption above, we can show the convergence of the approximate eigenpairs to the exact eigenpairs as $h\downarrow 0$ by means of the Rayleigh quotient techniques [19]. Error estimates are also obtainable if the eigenfunctions are sufficiently smooth. At first glance, the penalty method appears to be easy to apply. Actually, it appears to be difficult to find appropriate $\{V_i^h\}_{h>0}$ for Ω of general shape as we will see later by numerical results.

Before presenting concrete finite element models, we will give some preparations for the 2-D cases. Now we consider a domain Ω in $\boldsymbol{R}^2$ with Lipschitz continuous boundary $\partial\Omega$. Usually, we deal with bounded domains, but we also use unbounded ones for some auxiliary purposes. For 2-D vector-valued functions, we consider various function spaces as in the 3-D (three-dimensional) cases. Such function spaces are defined essentially in the same fashion as in the 3-D cases, and will be denoted by the same notations as in Section 2, but of course we must consider two-component vector-valued functions. In particular, we will often use $\{L_2(\Omega)\}^2$, whose norms and inner product are denoted by the

same notations $\|\cdot\|$ and $(,)$ as those of the scalar L_2-space for convenience. However, for the spaces related to the rotation operator, we should make some modifications since we must be careful in defining 2-D rotation operators. For this purpose, let us define two differential operators *rot* and *rot** by

$$\mathrm{rot}\, u=\partial u_2/\partial x_1-\partial u_1/\partial x_2\,,\qquad \mathrm{rot}^*\,\phi=\{\partial\phi/\partial x_2,\ -\partial\phi/\partial x_1\}\,, \tag{44}$$

where $u=\{u_1, u_2\}$ is a two-component vector function, ϕ is a scalar function, and $\{x_1, x_2\}$ is the variable of $\boldsymbol{R}^2$. Then $H(\mathrm{rot}\,;\Omega)$ and the related function spaces are defined as follows.

$$H(\mathrm{rot}\,;\Omega)=\{v\in\{L_2(\Omega)\}^2\,;\ \mathrm{rot}\, v\in L_2(\Omega)\}\ \text{equipped with}\ \|v\|_{H(\mathrm{rot}\,;\Omega)}=(\|v\|^2+\|\mathrm{rot}\, v\|^2)^{1/2}\,, \tag{45}$$

$$H_0(\mathrm{rot}\,;\Omega)=\{v\in H(\mathrm{rot}\,;\Omega)\,;\ (v, \mathrm{rot}^*\,\phi)=(\mathrm{rot}\, v, \phi)\ \text{for all}\ \phi\in H^1(\Omega)\}\,, \tag{46}$$

$$H(\mathrm{rot}^0\,;\Omega)=\{v\in H(\mathrm{rot}\,;\Omega)\,;\ \mathrm{rot}\, v=0\}=\{v\in\{L_2(\Omega)\}^2\,;\ (v, \mathrm{rot}^*\,\phi)=0\ \text{for all}\ \phi\in H_0^1(\Omega)\}\,, \tag{47}$$

$$H_0(\mathrm{rot}^0\,;\Omega)=\{v\in H_0(\mathrm{rot}\,;\Omega)\,;\ \mathrm{rot}\, v=0\}=\{v\in\{L_2(\Omega)\}^2\,;\ (v, \mathrm{rot}^*\,\phi)=0\ \text{for all}\ \phi\in H^1(\Omega)\}\,. \tag{48}$$

We do not define $H(\mathrm{rot}^*\,;\Omega)$ and $H_0(\mathrm{rot}^*\,;\Omega)$ since they are nothing but $H^1(\Omega)$ and $H_0^1(\Omega)$, respectively. We also employ the notations in (13). Some of the results in Section 2 are also valid in the 2-D cases. In particular, we have the following orthogonal decompositions of $\{L_2(\Omega)\}^2$:

$$\begin{aligned}\{L_2(\Omega)\}^2&=\mathrm{rot}^*\, H_0^1(\Omega)\oplus H(\mathrm{rot}^0\,;\Omega)=\mathrm{rot}^*\, H^1(\Omega)\oplus H_0(\mathrm{rot}^0\,;\Omega)\\&=\mathrm{rot}^*\, H_b^1(\Omega)\oplus \mathrm{grad}\, H^1(\Omega)\,,\end{aligned} \tag{49}$$

where $\mathrm{rot}^*\, H_0^1(\Omega)=\{\mathrm{rot}^*\,\phi\,;\ \phi\in H_0^1(\Omega)\}$, for example. For the last decomposition in (49), see [6].

Under the preparations above, we can consider the formulations in Section 3 even in the 2-D cases after necessary modifications. Moreover, Theorems 1 and 3 hold in the same forms. On the other hand, Theorem 2 does not hold in the original form. Instead, we have the following results frequently used in 2-D analyses.

THEOREM 4. *For $i=1, 2$, let us consider $\{\lambda, u\}\in\boldsymbol{R}^1\times U_i$ such that*

$$(\mathrm{rot}\, u, \mathrm{rot}\, v)=\lambda(u, v)\,;\quad \forall v\in U_i\,. \tag{50}$$

Then, if $\lambda\neq 0$, there exists $\phi\in W_{3-i}$ (i. e., $\phi\in W_2=H^1(\Omega)$ for $i=1$, and $\phi\in W_1=H_0^1(\Omega)$ for $i=2$) such that $\mathrm{rot}^*\,\phi=u$ *and*

$$(\mathrm{grad}\,\phi, \mathrm{grad}\,\phi)=\lambda(\phi, \phi)\,;\quad \forall\phi\in W_{3-i}\,. \tag{51}$$

Conversely, let us consider $\{\lambda, \phi\}\in \boldsymbol{R}^1\times W_{3-i}$ *that satisfies* (51). *Then* $u=\mathrm{rot}^*\,\phi$ *belongs to* U_i, *and* $\{\lambda, u\}$ *satisfies* (50).

Proof. We only prove the results for $i=1$, while we may prove those for $i=2$ in a similar fashion. For $\lambda\neq 0$, let us consider $u\in U_1=H_0(\mathrm{rot}\,;\Omega)$ that satisfies (50) for $i=1$. Then, we can find that such u is orthogonal to $H_0(\mathrm{rot}^0\,;\Omega)$ in $\{L_2(\Omega)\}^2$, and hence there exists a unique $\phi\in H^1(\Omega)$ such that $\mathrm{rot}^*\,\phi=u$ and $(\phi, 1)=0$ due to (49). Substituting this expression into (50) for $i=1$, we have

$$(\mathrm{rot}\,\mathrm{rot}^*\,\phi, \mathrm{rot}\,v)=\lambda(\mathrm{rot}^*\,\phi, v)=\lambda(\phi, \mathrm{rot}\,v)\quad \text{for all } v\in U_1\,. \tag{a}$$

For $\phi\in H^1(\Omega)$ with $(\phi, 1)=0$, let us consider $p\in H^1(\Omega)$ such that $(p, 1)=0$ and

$$(\mathrm{grad}\,p, \mathrm{grad}\,q)=(\phi, q)\quad \text{for all } q\in H^1(\Omega)\,.$$

Such a p exists uniquely, and $\mathrm{rot}^*\,p$ is in $U_1=H_0(\mathrm{rot}\,;\Omega)$ since $\mathrm{rot}\,\mathrm{rot}^*\,p=-\mathrm{div}\,\mathrm{grad}\,p=\phi\in H^1(\Omega)$ and $(\mathrm{rot}^*\,p, \mathrm{rot}^*\,q)=(\mathrm{grad}\,p, \mathrm{grad}\,q)=(\mathrm{rot}\,\mathrm{rot}^*\,p, q)$ for all $q\in H^1(\Omega)$. Substituting $v=\mathrm{rot}^*\,p$ into (a) and noting that $\mathrm{rot}^*\,\phi\in H_0(\mathrm{rot}\,;\Omega)$, we have

$$\begin{aligned}(\mathrm{rot}\,\mathrm{rot}^*\,\phi, \mathrm{rot}\,\mathrm{rot}^*\,p)&=(\mathrm{rot}\,\mathrm{rot}^*\,\phi, \phi)=(\mathrm{rot}^*\,\phi, \mathrm{rot}^*\,\phi)\\ &=\lambda(\phi, \mathrm{rot}\,\mathrm{rot}^*\,p)=\lambda(\phi, \phi)\,,\end{aligned}$$

and hence $(\mathrm{rot}^*\,\phi, \mathrm{rot}^*\,\phi)=(\mathrm{grad}\,\phi, \mathrm{grad}\,\phi)=\lambda(\phi, \phi)$. Since ϕ satisfies $(\phi, 1)=0$, (51) holds for any $\phi\in H^1(\Omega)$ which does not necessarily satisfy $(\phi, 1)=0$.

Conversely, let us consider $\phi\in H^1(\Omega)$ that satisfies (51) for $i=1$. Then, we have $\mathrm{rot}\,\mathrm{rot}^*\,\phi=\lambda\phi\in H^1(\Omega)$, and hence $u=\mathrm{rot}^*\,\phi$ belongs to $H(\mathrm{rot}\,;\Omega)$. Moreover, it holds for all $\phi\in H^1(\Omega)$ that

$$(\mathrm{rot}\,u, \phi)=\lambda(\phi, \phi)=(\mathrm{grad}\,\phi, \mathrm{grad}\,\phi)=(\mathrm{rot}^*\,\phi, \mathrm{rot}^*\,\phi)=(u, \mathrm{rot}^*\,\phi)\,,$$

which means that $u\in H_0(\mathrm{rot}\,;\Omega)$. Now, we have for any $v\in H_0(\mathrm{rot}\,;\Omega)$ that

$$(\mathrm{rot}\,u, \mathrm{rot}\,v)=\lambda(\phi, \mathrm{rot}\,v)=\lambda(\mathrm{rot}^*\,\phi, v)=\lambda(u, v)\,,$$

and the proof is complete. □

In 2-D cases, we usually use triangular or quadrilateral finite elements for triangulations. For simplicity, we assume that Ω is a bounded polygonal domain so that triangulation is always possible. Then, we approximate unknown functions by piecewise polynomials, and the isoparametric transformations are also available, see [2, 4]. When we use the penalty method, the functions to be approximated are in $H(\mathrm{rot}\,;\Omega)\cap H(\mathrm{div}\,;\Omega)$ so that the approximate functions should also belong to this space. Then it can be shown that the piecewise polynomial approximate functions must be continuous even across the interelement boundaries, and that such functions also belong to $\{H^1(\Omega)\}^2$, cf. Theorems 2.1.1 and 4.2.1 of [4]. Thus, so long as we use the present penalty approach, the approximate functions cannot be outside $\{H^1(\Omega)\}^2$. Moreover, we must impose boundary

conditions associated with the condition $u\in H_0(\mathrm{rot}\,;\Omega)$ $(i=1)$ or $u\in H_0(\mathrm{div}\,;\Omega)$ $(i=2)$. This may be done by introducing appropriate local coordinates as is commonly used in the finite element analysis [2]. In the next section, we will test the simplest finite element model based on this approach, and point out a numerical difficulty observed in a test problem.

Besides the formulations in Section 3, the formulations based on (51) in Theorem 4 are available for finite element analyses of the 2-D electromagnetic eigenvalue problem. Historically, such formulations are classical, and have been used almost exclusively in numerical analysis. This approach is essentially to approximate the eigenpairs of the Laplace operater with the homogeneous Neumann or Dirichlet boundary condition, and hence is fully established in the finite element method. In particular, all the standard Lagrange type elements for $H^1(\Omega)$ are available, and their approximation properties are also known [2, 4, 19]. In the next section, we will also use this approach to obtain reference numerical results.

The approximation capability of the penalty approach is not necessarily established for the standard piecewise polynomial approximations. However, in some special cases, we can prove it under mild assumptions on triangulations and finite elements. We first present the following lemma, which can be proved in a manner similar to that of the 3-D case [6, 10, 11].

LEMMA 1. *Let Ω be a bounded convex domain in $\boldsymbol{R}^2$. Then V_i is continuously imbedded in $\{H^1(\Omega)\}^2$ for $i=1, 2$. In other words,*

$$V_1=H_0(\mathrm{rot}\,;\Omega)\cap\{H^1(\Omega)\}^2\,,\qquad V_2=H_0(\mathrm{div}\,;\Omega)\cap\{H^1(\Omega)\}^2\,, \tag{52}$$

both algebraically and topologically.

Then we have the following theorem, by which we can prove the approximation capability of the standard piecewise polynomial finite element method based on the penalty approach when Ω is a bounded convex polygonal domain.

THEOREM 5. *When Ω is a bounded convex polygonal domain in $\boldsymbol{R}^2$, $V_i\cap\{C^\infty(\bar{\Omega})\}^2$ is dense in V_i $(i=1, 2)$, where $C^\infty(\bar{\Omega})$ is the totality of restrictions to Ω of infinitely differentiable functions defined in $\boldsymbol{R}^2$.*

Proof. We will only sketch the proof.

1. By the partition of unity for Ω, it is sufficient to consider functions with compact support and defined in the domain Ω^* shown in Fig. 1. More specifically, $\Omega^*\subset\boldsymbol{R}^2$ is defined by

$$\Omega^*=\{\{x_1, x_2\}\in\boldsymbol{R}^2\,;\ x_2>0,\ x_1>x_2\cot\theta\}\,,$$

where θ is an interior angle of Ω, which satisfies $0<\theta<\pi$ since Ω is convex. We should show that any $u\in V_i(\Omega^*)$ with compact support can be approximated

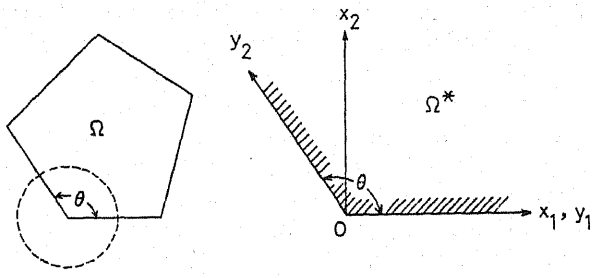

Fig. 1. Domains considered in the proof of Theorem 5.

by functions in $V_i(\Omega^*)\cap\{C^\infty(\overline{\Omega^*})\}^2$ $(i=1,2)$, where $V_i(\Omega^*)$ denotes V_i for Ω^*. By Lemma 1, u is actually in $V_i(\Omega^*)\cap\{H^1(\Omega^*)\}^2$.

2. We will first prove the results for $i=1$. Let us consider the coordinate transformation in $\boldsymbol{R}^2$ by

$$y_1=x_1-x_2\cot\theta\,,\qquad y_2=x_2/\sin\theta\,. \tag{a}$$

Then a point $\{x_1, x_2\}$ in Ω^* is mapped to a point $\{y_1, y_2\}$ in Ω^{**} defined by

$$\Omega^{**}=\{\{y_1, y_2\}\in\boldsymbol{R}^2\,;\ y_1>0,\ y_2>0\}\,.$$

For $u=\{u_1, u_2\}\in H_0(\mathrm{rot}\,;\Omega^*)\cap\{H^1(\Omega^*)\}^2$ with compact support, let us consider its *covariant* components $\{v_1, v_2\}$ in the oblique coordinates $\{y_1, y_2\}$. That is, with (a), v_1 and v_2 are defined by

$$v_1(y_1, y_2)=u_1(x_1, x_2)\,,\qquad v_2(y_1, y_2)=u_1(x_1, x_2)\cos\theta+u_2(x_1, x_2)\sin\theta\,.$$

We can easily show that v_1 and v_2 belong to $H^1(\Omega^{**})$ and have compact support. Moreover, from the condition $u\in H_0(\mathrm{rot}\,;\Omega^*)$, v_1 and v_2 are shown to satisfy, in the sense of trace, that

$$v_1(y_1, 0)=0\ \text{ for }\ y_1>0\,,\qquad v_2(0, y_2)=0\ \text{ for }\ y_2>0\,.$$

More specifically, we should notice that the condition $(u, \mathrm{rot}^*\,\phi)_{\Omega^*}=(\mathrm{rot}\,u, \phi)_{\Omega^*}$ for any $\phi\in H^1(\Omega^*)$ is equivalent to $(v, \mathrm{rot}^*\,\phi)_{\Omega^{**}}=(\mathrm{rot}\,v, \phi)_{\Omega^{**}}$ for any $\phi\in H^1(\Omega^{**})$, where $v=\{v_1, v_2\}$, $\mathrm{rot}\,v=\partial v_2/\partial y_1-\partial v_1/\partial y_2$, $\mathrm{rot}^*\,\phi=\{\partial\phi/\partial y_2, -\partial\phi/\partial y_1\}$, and $(\cdot,\cdot)_{\Omega^{**}}$ denotes the inner products of $L_2(\Omega^{**})$ and $\{L_2(\Omega^{**})\}^2$. Since v_1 and v_2 belong to $H^1(\Omega^{**})$, we can apply the Green formula to the above relation to obtain the conclusions.

Now we will use a kind of "reflection" technique. We extend $\{v_1, v_2\}$ to $\boldsymbol{R}^2$ by defining $\{w_1, w_2\}$ as follows.

$$\begin{aligned}
&w_1(y_1, y_2)=v_1(y_1, y_2)\,, && w_2(y_1, y_2)=v_2(y_1, y_2) && \text{if } y_1>0,\ y_2>0,\\
&w_1(y_1, y_2)=v_1(-y_1, y_2)\,, && w_2(y_1, y_2)=-v_2(-y_1, y_2) && \text{if } y_1<0,\ y_2>0,\\
&w_1(y_1, y_2)=-v_1(y_1, -y_2)\,, && w_2(y_1, y_2)=v_2(y_1, -y_2) && \text{if } y_1>0,\ y_2<0,\\
&w_1(y_1, y_2)=v_1(-y_1, -y_2)\,, && w_2(y_1, y_2)=v_2(-y_1, -y_2) && \text{if } y_1<0,\ y_2<0.
\end{aligned}$$

We may check that w_1 and w_2 have compact support and belong to $H^1(\boldsymbol{R}^2)$, by noting the continuity of traces along the lines $y_1=0$ and $y_2=0$. Then we can use the mollifier technique. That is, we first consider a non-negative C^∞-function $\rho(y_1, y_2)$ with compact support such that

$$\rho(-y_1, y_2)=\rho(y_1, y_2), \quad \rho(y_1, -y_2)=\rho(y_1, y_2), \quad \iint_{\boldsymbol{R}^2}\rho(y_1, y_2)dy_1dy_2=1,$$

and then approximate w_j $(j=1, 2)$ by

$$w_{\tau j}(y_1, y_2)=\tau^{-2}\int_{-\infty}^{\infty}\int_{-\infty}^{\infty} w_j(y_1-y_1^*, y_2-y_2^*)\rho(y_1^*/\tau, y_2^*/\tau)dy_1^*dy_2^*,$$

where τ is a positive parameter. Then $w_{\tau 1}$ and $w_{\tau 2}$ are C^∞-functions with compact support, and converge respectively to w_1 and w_2 in $H^1(\boldsymbol{R}^2)$ as $\tau\downarrow 0$. Noting the symmetry (or antisymmetry) of ρ, w_1, and w_2 in y_1 and y_2, we find that

$$w_{\tau 1}(y_1, 0)=w_{\tau 2}(0, y_2)=0 \quad \text{for } -\infty<y_1, y_2<\infty.$$

Now let us define the restrictions $v_{\tau j}$ of $w_{\tau j}$ to Ω^{**} $(j=1, 2)$, and then introduce a vector-valued function $u_\tau(x_1, x_2)$ which is defined in Ω^* and has $\{v_{\tau 1}, v_{\tau 2}\}$ as its covariant components in the oblique coordinates $\{y_1, y_2\}$. We can prove that u_τ belongs to $H_0(\mathrm{rot}\,; \Omega^*)\cap\{C^\infty(\overline{\Omega^*})\}^2$ and approximates u in the metric of $\{H^1(\Omega^*)\}^2$. This completes the proof for $i=1$.

3. The proof for $i=2$ may be given similarly. However, in this case, we use the *contravariant* components $\{v^1, v^2\}$ defined by

$$v^1(y_1, y_2)=u_1(x_1, x_2)-u_2(x_1, x_2)\cot\theta, \qquad v^2(y_1, y_2)=u_2(x_1, x_2)/\sin\theta.$$

Then v^1 and v^2 belong to $H^1(\Omega^{**})$, and, from the condition $u\in H_0(\mathrm{div}\,; \Omega^*)$, we have

$$v^1(0, y_2)=0 \quad \text{for } y_2>0, \qquad v^2(y_1, 0)=0 \quad \text{for } y_1>0.$$

The "reflection" technique is again used but in a different fashion. That is, v^1 is extended to be antisymmetric in y_1 and symmetric in y_2, while v^2 is extended to be symmetric in y_1 and antisymmetric in y_2. Then we can complete the proof by using the mollifier and restriction techniques as before. □

REMARK 3. By making full use of tensor analysis, we may extend the present results to the case where Ω is a bounded convex domain in $\boldsymbol{R}^2$ whose boundary consists of a finite number of sufficiently smooth arcs. However, it appears to be difficult to obtain the same results for general non-convex domains. Rather, our conjecture is that, for Ω of general shape, $V_i\cap\{H^1(\Omega)\}^2$ is not necessarily dense in V_i $(i=1, 2)$. If this is true, the use of the penalty finite element method based on piecewise polynomials appears to be hopeless for general purposes. It is known that V_i is not necessarily contained in $\{H^1(\Omega)\}^2$, see [20].

§ 5. Numerical results

For several 2-D problems, we test the simplest triangular finite element based on the penalty approach with the piecewise linear polynomial. We also use the piecewise linear triangular element for the eigenvalue problem (51) of the Laplace operator to obtain reference results. The latter method will be called the *conventional* one. We use the subspace iteration method to solve the arising algebraic eigenvalue problems [2]. Except it, we use standard computational techniques in the finite element analysis, and we omit the details here. As is shown in Fig. 2, we consider four types of domains: (1) rectangular domain, (2) circular domain, (3) pentagonal domain, (4) "curved" quadrilateral domain. In the actual computations, we only analyze the upper half portion of Ω as is hatched in the figure by taking advantage of the symmetric or antisymmetric properties of the eigenfunctions. Moreover, we deal with only a quarter part of Ω in the case of the circular domain.

Hereafter, we will only consider the problem corresponding to (1), which in the present case becomes

$$\text{rot}^* \text{rot}\, u=\lambda u \text{ and } \text{div}\, u=0 \quad \text{in } \Omega, \qquad u_t=0 \quad \text{on } \partial\Omega, \tag{53}$$

where $u=\{u_1, u_2\}$ is the electric field, and u_t is the tangential component of u on $\partial\Omega$. We solve (53) numerically by the proposed penalty finite element method with the value of ε usually taken as 1. On the other hand, the problem corresponding to (51) for $i=1$ is given by

$$-\text{div grad}\, \phi=\lambda\phi \quad \text{in } \Omega, \qquad \partial\phi/\partial n=0 \quad \text{on } \partial\Omega, \tag{54}$$

where $\partial\phi/\partial n$ represents the derivative of ϕ in the outward normal direction on $\partial\Omega$.

We numerically obtain the first (positive) eigenvalue and the associated eigenfunction of each problem. In the present case, the eigenfunction for the electric field u is expected to be symmetric with respect to the horizontal line passing through the barycenter of Ω, while that for the scalar function ϕ is expected to be antisymmetric. In addition, in the case of the circular domain,

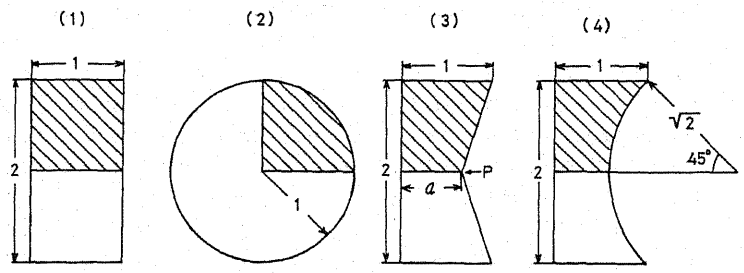

Fig. 2. Domains considered in numerical experiments.

the eigenfunctions u and ϕ are respectively expected to be antisymmetric and symmetric with respect to the vertical line passing through the center of Ω. We should impose appropriate numerical boundary conditions on the function values of u and ϕ at boundary nodes, although some of them may be dealt with as natural boundary conditions. At each node on the actual boundary $\partial\Omega$, the tangential value of u should be set equal to zero by using the local coordinate transformation technique [2], while we need not introduce any constraint on the value of ϕ. In particular, the values of both u_1 and u_2 should be set equal to zero at corner nodes on $\partial\Omega$ to match the condition $u_t=0$ in (53). However, if $\partial\Omega$ is curved, only the component of u in the actual tangential direction is set equal to zero, although $\partial\Omega$ is approximated by polygonal lines with nodes located on $\partial\Omega$ in such cases. Along the horizontal line passing through the barycenter, the nodal values of u_2 and ϕ are set equal to zero. On the other hand, along the vertical line passing through the center of the circular domain, only u_2 is set equal to zero.

5.1. *Problem* (1): *rectangular domain*

In this case, we use two types of meshes: mesh-1 and mesh-2 in Fig. 3. Approximate values for the first eigenvalue are given in Table 1 together with the results for other problems. They are fairly close to the exact one ($=\pi^2/4$ $=2.46740...$), and the convergence character appears to be reasonable. Figures 3 and 4 respectively show vector plots of the associated approximate eigenfunctions obtained by the conventional method (Fig. 3) and the penalty method (Fig. 4). The initial points of the arrows are the barycenters of triangles for the conventional method and the vertices of the triangles for the penalty method, respectively. Only the relative values of the arrow lengths are meaningful since eigenfunctions are considered. They coincide well with the exact eigenfunction expressed in terms of sinusoidal functions.

Table 1. Approximate results for the first eigenvalues

method	conventional		penalty ($\varepsilon=1$)		exact	condition at P
Problem	mesh-1	mesh-2	mesh-1	mesh-2		
(1)	2.4873	2.4724	2.4873	2.4724	2.4674	
(2)	3.4795	3.4122	3.3986	3.3932	3.3900	
(3) $a=0.5$	1.7746	1.7515	2.1603	2.1679	—	$u_2=0$
			6.1148	5.5463		$u_1=u_2=0$
(3) $a=1.8$	2.9005	2.8657	3.0865	2.9535	—	$u_2=0$
			3.1188	2.9617		$u_1=u_2=0$
(4)	1.9378	1.9220	2.0169	1.9422	—	

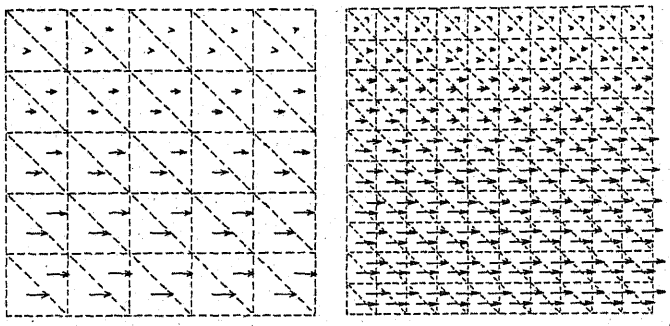

Fig. 3. Vector plots of the approximate eigenfunctions. (Problem (1), conventional)

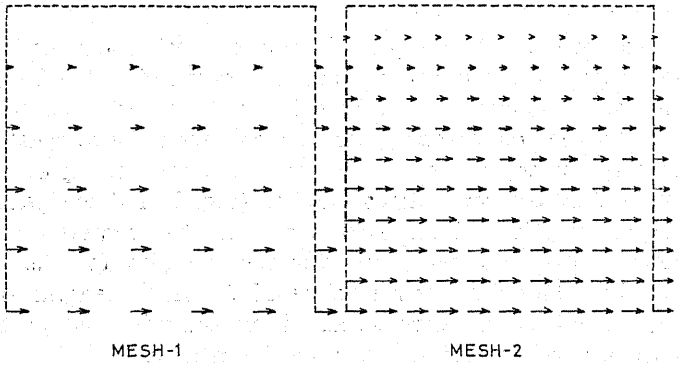

Fig. 4. Vector plots of the approximate eigenfunctions. (Problem (1), penalty)

To see the influence of ε on the numerical solutions based on the penalty method, we obtain eigenvalues for mesh-1 numerically by changing ε in the interval $0<1/\varepsilon\leqq 0.5$. The results are summarized in Fig. 5. We can see that there are many small eigenvalues when $1/\varepsilon$ is close to zero. This type of numerical phenomenon is known as the *spectral pollution* [7]. However, as $1/\varepsilon$ increases, most of the non-physical eigenvalues grow rapidly and only physically meaningful approximate eigenvalues remain to be almost constant. Here, the "physically meaningful" eigenvalues are those whose associated eigenfunctions satisfy the divergence-free condition approximately. In the present figure, only one approximate eigenvalue is insensitive to the variation of ε, and is close to the exact first eigenvalue. Thus, we have numerically confirmed the observations suggested by Theorem 3: we need not use too small values of ε if we are interested in only restricted number of eigenvalues close to zero.

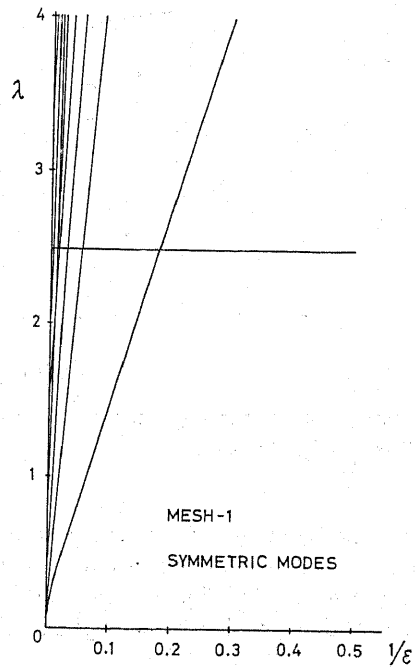

Fig. 5. Variation of the approximate eigenvalues against ε. (Problem (1), penalty, mesh-1)

5.2. *Problem* (2): *circular domain*

The employed mesh patterns are shown in Fig. 6, and approximate values for the first eigenvalue are given in Table 1. The exact eigenvalue and the

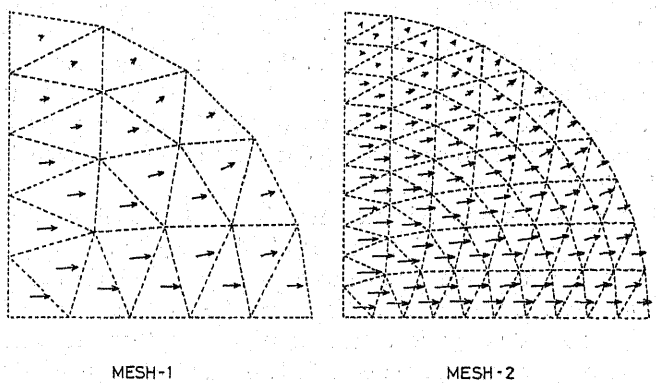

Fig. 6. Vector plots of the approximate eigenfunctions. (Problem (2), conventional)

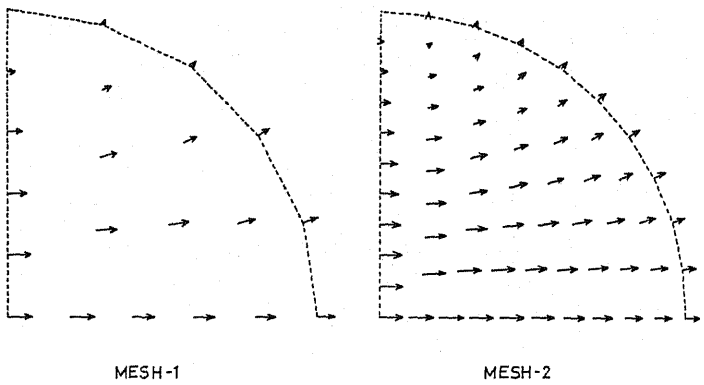

Fig. 7. Vector plots of the approximate eigenfunctions. (Problem (2), penalty)

associated eigenfunction may be obtained by the use of the Bessel function. Vector plots of approximate eigenfunctions are drawn in a similar manner to that of Problem (1) and are given in Fig. 6 (conventional method) and Fig. 7 (penalty method). Again, the approximate eigenpairs coincide fairly well with the exact one.

5.3. *Problem* (3): *pentagonal domain*

As the third problem, we consider a pentagonal domain shown in Fig. 2, where a is a geometric parameter indicating the length of the horizontal segment passing through the barycenter of Ω. We use two types of meshes: mesh-2 is shown in Figs. 9 and 11, while mesh-1, not shown here, is similar to mesh-1 of Problem (1). We should take a special care of the nodal value of u at corner point P shown in the figure, since P becomes a point of reentrant corner when $a<1$. To match with the boundary condition in (53), nodal values of both u_1 and u_2 should be set equal to zero at P. However, we also use the procedure introduced by Hara in [8, 14] to deal with this reentrant corner which may produce strong singularity to the eigenfunctions: we set only the nodal value of u_2 to zero at P, while we make the nodal value of u_1 unconstrained. Such a procedure is not justified theoretically, but may brings us some improvements to numerical solutions as we will see soon.

Fig. 8 illustrates the approximate first eigenvalues against a ($0.3 \leqq a \leqq 1.8$). We can readily see that the eigenvalues obtained by the penalty method with $u_1=u_2=0$ at P are quite larger than those of other methods especially when a is smaller. On the other hand, the results by the conventional method appear to be generally reasonable. It is theoretically known that the conventional method gives convergent approximate solutions, and the obtained approximate eigenvalues are upper bounds of the exact ones [19]. When the numerical boundary condition at P is modified as was mentioned before, the results improve

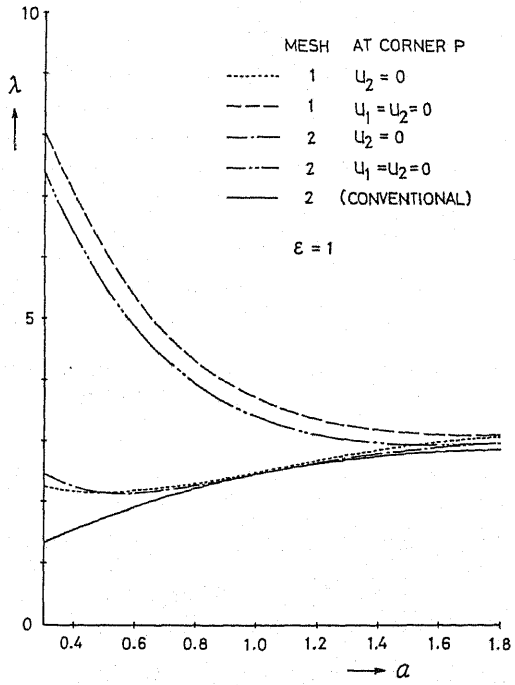

Fig. 8. Variation of the approximate eigenvalues against a. (Problem (3))

but are not fully reasonable when $a<1$. In particular, the accuracy is not necessarily improved but becomes worse by mesh refinement when a is close to 0.3. It is also to be noted that the differences of the approximate values are not so large when a is close to 1.8.

Figures 9 and 10 show the vector plots of approximate eigenfunctions for

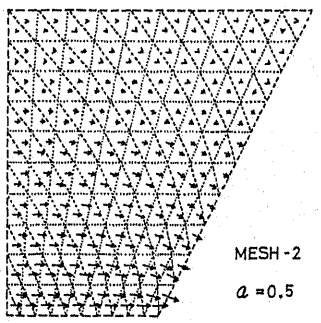

Fig. 9. Vector plots of the approximate eigenfunction. (Problem (3), $a=0.5$, conventional, mesh-2)

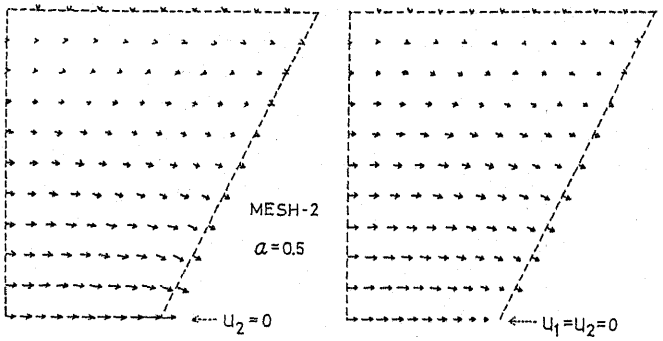

Fig. 10. Vector plots of the approximate eigenfunctions. (Problem (3), α=0.5, penalty, mesh-2)

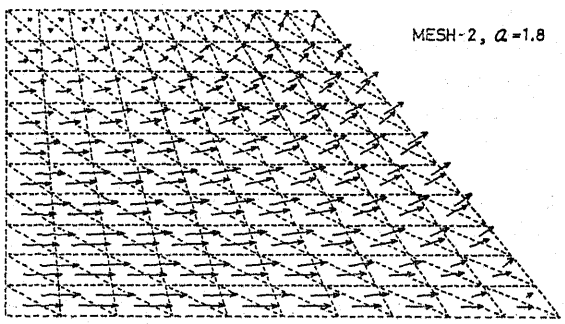

Fig. 11. Vector plots of the approximate eigenfunction. (Problem (3), α=1.8, conventional, mesh-2)

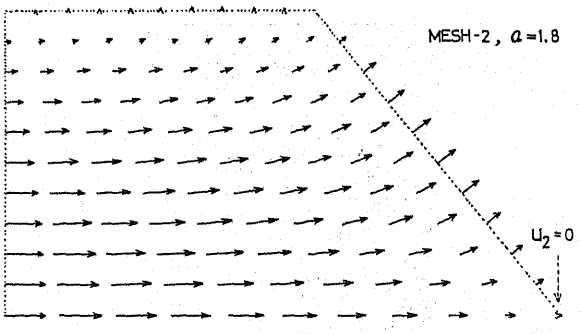

Fig. 12. Vector plots of the approximate eigenfunction. (Problem (3), α=1.8, penalty, mesh-2, u_2=0 at P)

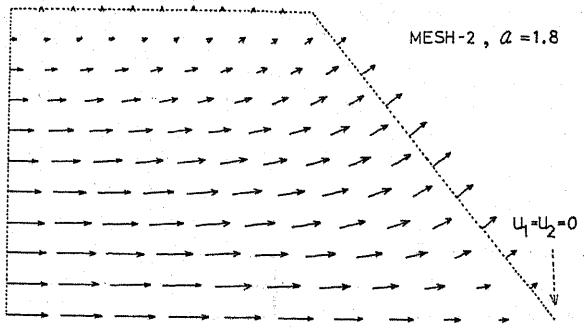

Fig. 13. Vector plots of the approximate eigenfunction.
(Problem (3), $\alpha=1.8$, penalty, mesh-2, $u_1=u_2=0$ at P)

$\alpha=0.5$ by the conventional method and the penalty method, respectively. We can see that the singularity of u at P is not well represented by the penalty method. Figures 11 to 13 show similar results for $\alpha=1.8$. In this case, the differences of numerical solutions are not so large. Notice that it is theoretically shown in Section 4 that the penalty finite element method can give convergent numerical solutions in the present case where Ω is a convex bounded polygonal domain.

5.4. *Problem* (4): *"curved" quadrilateral domain*

As the final problem, we consider a quadrilateral domain, one side of which is a circular arc. In this case, Ω is not convex, but does not have reentrant corners. Employed meshes are shown in Fig. 14.

Unlike in Problem (3), the approximate eigenvalues given in Table 1 agree farly well with each other and appear to be convergent in all the cases. The

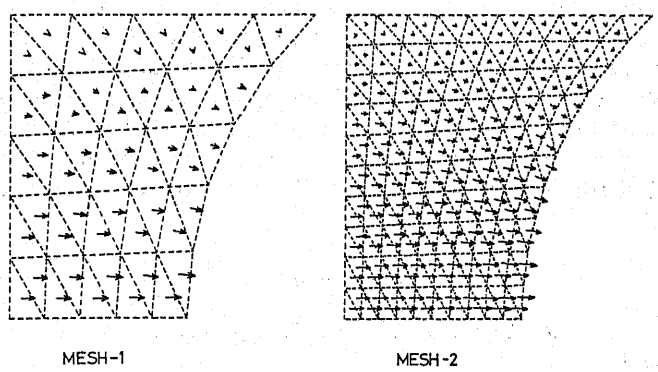

Fig. 14. Vector plots of the approximate eigenfunctions.
(Problem (4), conventional)

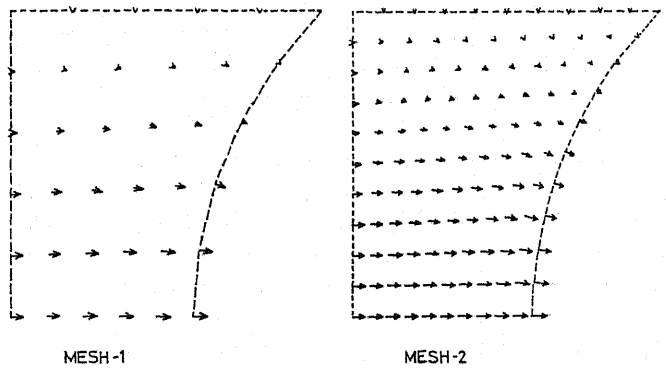

Fig. 15. Vector plots of the approximate eigenfunctions. (Problem (4), penalty)

vector plots of approximate eigenfunctions are illustrated in Fig. 14 (conventional method) and Fig. 15 (penalty method), and agree well with each other. Thus, the penalty method appears to be applicable to the present problem in which no reentrant corner exists, though the convergence may not be so rapid as in the convex cases.

§ 6. Concluding remarks

We have presented some weak formulations for an electromagnetic eigenvalue problem related to free vibration analysis of cavity resonators and wave guides. Some of the theoretical results were already published in [12], but we give here complete proofs to them and add some new results. We also test the penalty approach more systematically than in [8, 14], and point out a numerical difficulty when the penalty approach is applied to problems on domains with reentrant corners. On the other hand, the mixed method given in [9, 12] appears to be free from such a difficulty. At present, Hypotheses [H1] and [H2] employed in this paper are not shown to be true except for some special domains. Moreover, the problem given at the end of Section 4 appears to be open. Thus there are many things left to be done from both theoretical and numerical viewpoints. Since the present eigenvalue problem is of much practical importance, we will continue our theoretical studies to solve such open problems.

References

[1] Atwater, H. A., *Introduction to Microwave Theory*, McGraw-Hill Pub. Co. (New York, 1962), Ch. 3.

[2] Bathe, K.-J., and Wilson, E. L., *Numerical Methods in Finite Element Analysis*, Prentice-Hall, Inc. (Englewood Cliffs, 1976).

[3] Brezzi, F., On the existence, uniqueness and approximation of saddle point problems arising from Lagrangian multipliers, *RAIRO*, **8**, 129–151 (1974).
[4] Ciarlet, P.G., *The Finite Element Method for Elliptic Problems*, North-Holland Pub. Co. (Amsterdam-New York-Oxford, 1978).
[5] Duvaut, G., and Lions, J.L., *Inequalities in Mechanics and Physics*, Springer Verlag (Berlin-Heidelberg-New York, 1976), Ch. 7.
[6] Girault, V., and Raviart, P.-A., *Finite Element Methods for Navier-Stokes Equations, Theory and Algorithms*, Springer-Verlag (Berlin-Heidelberg-New York-Tokyo, 1986), Ch. 1.
[7] Gruber, R., and Rappaz, J., *Finite Element Method in Linear Ideal Mganetohydrodynamics*, Springer-Verlag (Berlin-Heidelberg-New York, 1985).
[8] Hara, M., Wada, T., Fukasawa, T., and Kikuchi, F., Calculation of RF electromagnetic field by finite element method (II), *RIKEN (Institute of Physical and Chemical Research) Accelerator Progress Report*, **16**, 227–229 (1982).
[9] Hara, M., Wada, T., Mitomori, K., and Kikuchi, F., Three dimensional analysis of RF electromagnetic field by the finite element method, in *Proc. 11-th Int. Conf. Cyclotron and their Applications*, Oct. 13–17, 1986, Tokyo (M. Sekiguchi, Y. Yano, and K. Hatanaka, Eds.), IONICS Pub. Co. (Tokyo, 1987), pp. 337–340.
[10] Kaizu, S., and Kikuchi, F., An imbedding theorem for a Hilbert space appearing in electromagnetics, *Sci. Papers College Arts Sci., Univ. Tokyo*, **36**, 81–89 (1986).
[11] Kikuchi, F., An isomorphic property of two Hilbert spaces appearing in electromagnetism: analysis by the mixed formulation, *Japan J. Appl. Math.*, **3**, 53–58 (1986).
[12] Kikuchi, F., Mixed and penalty formulations for finite element analysis of an eigenvalue problem in electromagnetism, *Computer Meth. Appl. Mech. Eng.*, **64**, 509–521 (1987).
[13] Kikuchi, F., Mixed formulations for finite element analysis of magnetostatic and electrostatic problems, to apear in *Japan J. Appl. Math.*, **6**, (1989).
[14] Kikuchi, F., Hara, M., Wada, T., and Nakahara, K., Calculation of RF electromagnetic field by finite element method (III), *RIKEN (Institute of Physical and Chemical Research) Accelerator Progress Report*, **17**, 153–155 (1983).
[15] Leis, R., Zur Theorie elektromagnetischer Schwingungen in anisotropen inhomogenen Medien, *Math. Z.*, **106**, 213–224 (1968).
[16] Nedelec, J.-C., Mixed finite elements in $\boldsymbol{R}^3$, *Numer. Math.*, **35**, 315–341 (1980).
[17] Nedelec, J.C., A new family of mixed finite elements in $\boldsymbol{R}^3$, *Numer. Math.*, **50**, 57–81 (1986).
[18] Neittaanmaki, P., and Saranen, J., On the finite element approximation for Maxwell's problem on polygonal domains, *Int. J. Appl. Anal.*, **12**, 73–83 (1981).
[19] Strang, G., and Fix, G.J., *An Analysis of the Finite Element Method*, Prentice-Hall, Inc. (Englewood Cliffs, 1973), Ch. 6.
[20] Weck, N., Maxwell's boundary value problem on Riemannian manifolds with nonsmooth boundaries, *J. Math. Anal. Appl.*, **46**, 410–437 (1974).